

General Disclaimer

One or more of the Following Statements may affect this Document

- This document has been reproduced from the best copy furnished by the organizational source. It is being released in the interest of making available as much information as possible.
- This document may contain data, which exceeds the sheet parameters. It was furnished in this condition by the organizational source and is the best copy available.
- This document may contain tone-on-tone or color graphs, charts and/or pictures, which have been reproduced in black and white.
- This document is paginated as submitted by the original source.
- Portions of this document are not fully legible due to the historical nature of some of the material. However, it is the best reproduction available from the original submission.

(NASA-CR-152737) PREDICTION OF SKYLAB
ATTITUDE MOTION FOR SPACE SHUTTLE REVISIT
(Pennsylvania State Univ.) 29 p HC A03/MF
A01

CSCI 22A

N77-21108

Unclas

G3/12 24328

ABSTRACT

One of NASA's primary mission objectives for its first flights of the Space Shuttle System is to revisit the Skylab vehicle. The purpose of this revisit will be to add a kick stage to the vehicle to raise its orbit and to do a limited number of experiments. Without the addition of the kick motor Skylab's orbit will decay by mid-1980. Unfortunately, it is highly likely that the Skylab will be in a tumbling mode, because it is not controlled and it is under the influence of environmental effects. The work reported in the proposed paper deals with the prediction of this uncontrolled motion. Computer simulations were employed to generate results based on a fairly complicated analytical model. Environmental effects considered include atmospheric drag and gravity gradients. Mathematical models were based on Euler's moment equations and transformations from the body frame to inertial frame. A range of altitudes was considered, from 278 kilometers to 417 kilometers. Skylab is predicted to be in this orbital range during the 1979-1980 period. Results indicated that there will be a cyclic attitude motion due to the combined effect of gravity gradient and atmosphere drag. This motion can be characterized as being a slow tumble. A three-degree-of-freedom simulator is used to show what the space shuttle crew will see as they approach the Skylab.

NOMENCLATURE

$A, B, C,$	Satellite principal moments of inertia
A_{ref}	Skylab reference area
$A_1, B_1, A_{1j},$ B_{1j}	Fourier Series coefficients
C_x, C_y, C_z	Skylab roll, pitch, and yaw aerodynamic drag moment coefficients
D_{ref}	Skylab reference diameter
M_x, M_y, M_z	External moments on satellite
M_{gx}, M_{gy}, M_{gz}	Gravity gradient moments
M_{ax}, M_{ay}, M_{az}	Aerodynamic moments
q	Dynamic pressure - $1/2 \rho v^2$
R	Satellite distance from earth's center
V_o	Satellite orbital velocity
V	Satellite velocity relative to the incident stream
X_I, Y_I, Z_I	Geocentric inertial coordinate system
X_b, Y_b, Z_b	Body coordinate system
α_a	Satellite angle of attack
μ	Earth's gravitational constant
ϕ_a	Satellite roll angle
ρ	Atmospheric density
ρ_A, ρ_B	Density cosine curve fit constants
ψ, θ, ϕ	Euler Angles
$\dot{\psi}, \dot{\theta}, \dot{\phi}$	Euler Rates
ω	Satellite angular velocity
$\dot{\omega}$	Satellite angular acceleration

CHAPTER 1

Introduction

1.1 Origin and Importance of Investigation

A revisit to the Skylab spacecraft is one of the early priority missions NASA envisions for the Space Shuttle. Currently Skylab is in a decaying orbit around the earth such that by late 1979-1980 it will enter the atmosphere and burn up. The purpose of the Space Shuttle visit would be to add a kick stage to Skylab to raise its orbit so it could be used for further experimentation. However, Skylab is now passive and is under the influence of environmental perturbations which cause it to tumble. Skylab must be motionless in order that work may be done on the vehicle. Therefore, an idea of what Skylab will look like as the Space Shuttle crew approaches is necessary so that proper and adequate equipment to slow or stop the tumble can be placed on board the Shuttle.

1.2 Statement of the Problem and Scope of Investigation

The purpose of this investigation, then, is to predict Skylab's attitude motion in 1979-1980. Various perturbation forces acting on the passive vehicle are considered and numerically analyzed. These expressions are incorporated into Euler's moment equations and then solved via a digital computer. The moment equations are solved for four altitudes ranging from 278 kilometers to 417 kilometers since orbital decay prediction for Skylab shows this range of altitude for Skylab's orbit at the time of the Shuttle visit. The resulting solutions show cyclic tumbling. A three-degree-of-freedom simulator is used to visualize the predicted motion of Skylab.

This investigation lays groundwork for NASA to decide if a Skylab revisit is feasible. It also provides information that can be of great importance for predicting other satellite tumbling modes so that they, too, may be revisited and reactivated.

CHAPTER 2

Background Information

2.1 Coordinate Systems

In order to begin a study of the motion of a satellite, a coordinate system to describe the position and attitude of the satellite must be established. Two such systems are here defined.

2.1.1 Inertial Reference Coordinate System

Figure 1 depicts the standard geocentric inertial coordinate system. It has its origin at the earth's center with the $X_I - Y_I$ plane coinciding with the earth's equatorial plane and X_I pointing toward the Vernal Equinox. The inertial reference coordinate is denoted in matrix form

$$\begin{bmatrix} X_I \\ Y_I \\ Z_I \end{bmatrix}.$$

2.1.2 Satellite Body Coordinate System

Body coordinates,

$$\begin{bmatrix} x_b \\ y_b \\ z_b \end{bmatrix},$$

are related to inertial coordinates through the Euler angles ψ , θ , ϕ as shown in figure 2. The transformation matrix for inertial to body coordinates is derived in reference (1) as:

$$\begin{bmatrix} x_b \\ y_b \\ z_b \end{bmatrix} = \begin{bmatrix} (\cos \phi \cos \psi - \sin \phi \cos \theta \sin \psi) \\ (-\sin \phi \cos \psi - \cos \phi \cos \theta \sin \psi) \\ (\sin \theta \sin \psi) \end{bmatrix}$$

$$\begin{bmatrix} (\cos \phi \sin \psi + \sin \phi \cos \theta \cos \psi) & (\sin \phi \sin \theta) \\ (-\sin \phi \sin \psi + \cos \phi \cos \theta \cos \psi) & (\cos \phi \sin \theta) \\ (-\sin \theta \cos \psi) & (\cos \theta) \end{bmatrix} \begin{bmatrix} x_I \\ y_I \\ z_I \end{bmatrix}$$

(2.1.2-1)

Of special interest to this investigation is the transformation that relates the Euler rates to a body angular velocity vector, ω , also shown in Figure 2. This transformation matrix is found in reference (1) as:

$$\begin{bmatrix} \dot{\psi} \\ \dot{\theta} \\ \dot{\phi} \end{bmatrix} = \frac{1}{\sin \theta} \begin{bmatrix} \sin \phi & \cos \phi & 0 \\ \cos \phi \sin \theta & -\sin \phi \sin \theta & 0 \\ -\sin \phi \cos \theta & -\cos \phi \cos \theta & \sin \theta \end{bmatrix} \cdot \begin{bmatrix} \omega_x \\ \omega_y \\ \omega_z \end{bmatrix} \quad (2.1.2-2)$$

2.2 Equations of Motion

In reference (1), Euler's equations of motion for principal axes are given as:

$$M_x = A \dot{\omega}_x + \omega_y \omega_z (C-B) \quad (2.2-1a)$$

$$M_y = B \dot{\omega}_y + \omega_x \omega_z (A-C) \quad (2.2-1b)$$

$$M_z = C \dot{\omega}_z + \omega_x \omega_y (B-A) \quad (2.2-1c)$$

Where A, B, and C are the principal moments of inertia coinciding with the principal body axes x, y, and z, ω is the angular velocity, and $\dot{\omega}$ is the angular acceleration. It is important to note that equations (2.2-1) are expressed in body coordinates.

CHAPTER 3

Discussion, Analysis, and Reduction of External Moments

Reduction of environmental perturbation moment expressions to a manageable form requires theoretical analysis to determine which outside forces are small and can be neglected without loss of accuracy. The following deals with discussion and reduction of the four principal perturbing forces--gravity gradient, atmospheric drag, solar radiation, and magnetic torques--so that these forces can be incorporated into a digital program to determine Euler angles and rates.

3.1 Gravity Gradient

The gravitational attraction between the enormous mass of the earth and a satellite in a fairly close orbit about the earth produces a torque which is a major perturbation of the attitude of the satellite. The gradient of the gravity force produces this perturbation. The gravity gradient is a function of satellite altitude, satellite orientation, earth mass distribution, and satellite mass distribution.

By assuming a spherical earth of relatively uniform mass distribution, and by assuming that the satellite is a point mass as compared to the mass of the earth, expressions for the moments produced from the gravity gradients are illustrated by Tate in reference (2) as follows:

$$M_{gx} = \frac{3\mu}{2R^2} \sin 2\phi \cos^2 \theta (C-B) \quad (3.1-1a)$$

$$M_{gy} = \frac{3\mu}{2R^2} \sin 2\theta \cos \phi (C-A) \quad (3.1-1b)$$

$$M_{gz} = \frac{3\mu}{2R^2} \sin 2\theta \sin \phi (A-B) \quad (3.1-1c)$$

One important note is that equations (3.1-1) are derived and written in body coordinates, and R is the distance from the center of the earth (the origin of the geocentric coordinate system) to the satellite center of mass. Values of A , B , and C , the satellite principal moments of inertia, are given in appendix A.

3.2 Aerodynamic Drag

Around the year 1980, Skylab will be orbiting at an altitude of less than 350 kilometers. Aerodynamic drag, a function of atmospheric density, satellite velocity, satellite shape, and satellite angle of attack, becomes a major external perturbation force at altitudes of 800 kilometers or less. Therefore, in this investigation, aerodynamic drag moments must be considered. Following the format in reference (2), external moments due to aerodynamic drag are found to be:

$$M_{ax} = c_z q A_{ref} D_{ref} \quad (3.2-1a)$$

$$M_{ay} = c_y q A_{ref} D_{ref} \quad (3.2-1b)$$

$$M_{az} = c_z q A_{ref} D_{ref} \quad (3.2-1c)$$

where c_x is the roll moment coefficient, c_y is the pitch moment coefficient, c_z is the yaw moment coefficient, A_{ref} is the Skylab reference area, D_{ref} is the Skylab reference diameter, q is the dynamic pressure, $\frac{1}{2} \rho V_o^2$, and V_o is the orbital velocity.

Aerodynamic drag depends upon atmospheric density, ρ , and the pitch, roll, and yaw moment coefficients. However, density is a function not only of altitude but also of other variations that change with time. The moment coefficients vary with time due to Skylab's changing attitude. In order to accommodate these time dependent variations, density and moment coefficients must be handled separately and then incorporated into the atmospheric drag moment expressions.

Interpolation of information from the chart of Figure 3 indicates that Skylab will be within 278 to 417 kilometers above the earth during the time in question (1979-1980). Therefore, four representative altitudes of 278, 324, 370, and 417 kilometers were chosen. Evaluations of all perturbations were made at these four altitudes in order to produce a more general overview of the probable motion of Skylab.

3.2.1 Density Evaluation

Since the possible orbital altitudes of Skylab are well over 90 kilometers, the Jacchia (1970) model for atmospheric density at satellite altitudes was chosen to evaluate the density variations of the orbits. The Jacchia model in its completeness accounts for temperature and density variations due to seasonal and latitudinal variations, to both solar and geomagnetic activity, and diurnal and semi-annual variations. A copy of the basic Jacchia program

is found in reference 4. The Jacchia model program as supplied by NASA had to be slightly reworked and adapted to fit the constraints of the IBM 370/168 computer used at The Pennsylvania State University.

The Jacchia model will calculate density values every minute, every day. In order to reduce computer time, noon March, 1980 was chosen as an average reference time to represent early 1980. The solar indices for this date were obtained from NASA. The density distribution about the earth was then calculated using the Jacchia program. This distribution was modelled to represent a cosine curve illustrating the higher density values on the sunside of the earth. These cosine curve fits generally were accurate to within five percent of the actual calculated values. The density distribution about the earth could then be obtained from the following equation:

$$\rho = \rho_B + \rho_A \cos (\omega_0 t) \quad (3.2.1-1)$$

The values of ρ_A , ρ_B and ω_0 for each reference altitude are given in appendix A. The variable t in equation (3.2.1-1) is time, where the time relates to the longitudinal position in the orbit.

3.2.2 Moment Coefficient Evaluation

A Fourier series curve fit formula, obtained from NASA by Tate (2), calculates the aerodynamic drag moment coefficients as functions of the satellite angle of attack, α_a , and the roll angle, ϕ_a , as shown in Figure 4.

The drag coefficient equation is:

$$C(\alpha_a, \phi_a) = \frac{A_0}{2} (\phi_a) + \sum_{i=1}^m [A_i (\phi_a) \cos i \alpha_a + B_i (\phi_a) \sin i \alpha_a] \quad (3.2.2-1)$$

$$A_i(\phi_a) = \frac{a_{aio}}{2} + \sum_{j=1}^n [a_{aij} \cos j \phi_a + b_{aij} \sin j \phi_a] \quad (3.2.2-2)$$

$$B_i(\phi_a) = \frac{a_{bio}}{2} + \sum_{j=1}^n [a_{bij} \cos j \phi_a + b_{bij} \sin j \phi_a] \quad (3.2.2-3)$$

Fourier series analysis leads to the finding that coefficients evaluated at $i = 1, 3$ and $j = 2, 4, 6$ and coefficients evaluated at $i = 1, 3$, and $j = 1, 3, 5$, yield a highly accurate representation of the coefficient curve.

The $a_{ij} A_i$, $b_{ij} A_i$, $a_{ij} B_i$ and $b_{ij} B_i$ coefficient values are given in Tate (2). These coefficient values are based on Skylab with the auxiliary thermal shield, ATM solar arrays, and orbital workshop solar panel No. 1 deployed as shown in Figure 4.

The angles ϕ_a and α_a are evaluated in body coordinates such that

$$\phi_a = \tan^{-1} \left[\frac{\frac{V_y}{V_z}}{\frac{V_x}{V_z}} \right]_b, \quad 0^\circ \leq \phi_a \leq 360^\circ \quad (3.2.2-4)$$

$$\alpha_a = \cos^{-1} \left[\frac{\frac{V_x}{V}}{\frac{V_z}{V}} \right]_b, \quad 0^\circ \leq \alpha_a \leq 180^\circ \quad (3.2.2-5)$$

Since the orbit of Skylab is assumed circular, $V = V_0$ where V_0 is given in body coordinates by

$$V_x = V_o \cos \theta \cos \psi \quad (3.2.2-6a)$$

$$V_y = V_o \sin \phi \sin \theta \cos \psi - \cos \phi \sin \psi \quad (3.2.2-6b)$$

$$V_z = V_o \cos \phi \sin \theta \cos \psi + \sin \phi \sin \psi \quad (3.2.2-6c)$$

The equations for calculating the aerodynamic moment coefficients, c_x , c_y , and c_z , were written into a separate subroutine to be used in the subroutine to calculate total aerodynamic drag moments

3.2.3 Complete Subroutine for Aerodynamic Drag

The first part of the subroutine to calculate aerodynamic drag at the reference altitudes incorporated the cosine curve fit equations as a function of height and time. The second part consisted of the subroutine to calculate the moment coefficients as a function of velocity, angle of attack, and roll angle, as well as the reference area, A_{ref} , and the reference diameter, D_{ref} , as given in Appendix A. By incorporating equations (3.2-1) and the expression for aerodynamic pressure, $q = \frac{1}{2} \rho V_o^2$, the expressions for aerodynamic moments are obtained as

$$M_{ax} = \frac{1}{2} \rho c_x A_{ref} D_{ref} V_o^2 \quad (3.2.3-1a)$$

$$M_{ay} = \frac{1}{2} \rho c_y A_{ref} D_{ref} V_o^2 \quad (3.2.2-1b)$$

$$M_{az} = \frac{1}{2} \rho c_z A_{ref} D_{ref} V_o^2 \quad (3.2.2-1c)$$

in body coordinates.

3.3 Solar Wind Radiation

The sun produces radiation which will strike a body in space and impart momentum to that body. The amount of momentum transferred to the body in the form of torques depends on the distance the body is from the sun, the body surface geometry, and the body surface reflectivity. Examination of the moments due to solar wind and solar radiation indicate that their effect on Skylab will remain negligible. Since solar effects are relatively small at low altitudes and since the solar moment expression is difficult to handle numerically, the effect of solar moments can be neglected while still achieving a good deal of accuracy in the modelling of Skylab's attitude motion.

3.4 Magnetic Torques

A satellite's magnetic components interact with the earth's magnetic field causing perturbation torques on the satellite. However, since Skylab is passive, the magnetic interaction between it and the earth are assumed negligible, and are not included in this investigation.

3.5 Final Moment Equations

The final moment equations that were numerically integrated are found by combining equations (3.1-1) and (3.2.3-1) with equation (2.2-1) such that

$$M_{gx} + M_{ax} = A \dot{\omega}_x + \omega_y \omega_z \quad (C-B) \quad (3.5-1a)$$

$$M_{gy} + M_{ay} = A \dot{\omega}_y + \omega_x \omega_z \quad (A-C) \quad (3.5-1b)$$

$$M_{gz} + M_{az} = A \dot{\omega}_z + \omega_x \omega_y \quad (B-A) \quad (3.5-1c)$$

CHAPTER 4

Results

Euler's equations of motion, equations (3.5-1), were solved numerically using an IBM 370/168 digital computer. The external moments were calculated by the methods described in Chapter 3. The integration routine consisted of a second order Runge-Kutta method used for the first four iterations to start the solution. The routine then switched to a Hamming predictor-corrector method for the remainder of the program. A time increment of five seconds was used.

The input for the program was the initial Euler angles, the orbital altitude, the density model and constants, and the Fourier aerodynamic moment model and constants. The input can be found in appendix A. The output of the integration routine was the body rates and their time derivatives as functions of time. Equation (2.1.2-2) was then used to transform the body rates to the final output, the Euler rates. Using a more standard notation the body, x, y, and z rates may be respectively denoted as the yaw, roll, and pitch rates with respect to the orbital plane as shown in Figure 5.

Figures 6 through 9 are plots of the precession, nutation and spin rates as functions of time for each of the four altitudes considered. After one orbital period, all precession and spinning motion show cyclic tumbling characteristic of gravity gradient perturbation. The nutation motion lacks this cyclic behavior because there is no gradient of gravitational force in this mode. This can be seen in the relatively slow increase and small nutation rate which implies only aerodynamic torques affect this mode.

The singular points in the precession and spin rates are caused by θ the nutation angle, approaching zero. The transformation used, equation (2.1.2-2), has a factor of $\frac{1}{\sin \theta}$ which causes singularity for θ approaching zero. In the case of the 324 kilometer plots, θ actually passes through zero, delaying the cyclic tumbling in the precession and spin rates.

Examination of the plots for 278 kilometers, Figure 6, shows that the precession and spin rates reach a steady state tumbling motion after about one orbital period, approximately 92 minutes. Ignoring the singular points, the rates and periods of this steady state motion are:

$\dot{\psi}$, Precession rate:	Period = 40 minutes
	Rates = $-.8$ to $.8$ degrees/second
$\dot{\theta}$, Nutation rate:	Motion is not cyclic
	Rates = $-.4$ to $.4$ degrees/second
$\dot{\phi}$, Spin rate:	Period = 40 minutes
	Rates = $-.5$ to $.5$ degrees/second

A three degree of freedom simulator was used to better visualize the attitude motion. The Euler rates obtained from the digital computer were transformed to DC voltage using a digital to analog converter. These voltages then fed the motors which ran the gimbals of the simulator. The configuration is shown in Figure 10.

REFERENCES

1. Kaplan, Marshall H., Modern Spacecraft Dynamics and Control, John Wiley and Sons., Inc., New York, 1976, pp. 8-13,50.
2. Tate, Vincent, "Investigation of Environmental Perturbations on a Passive Asymmetric Satellite," Astronautics Research Report Number 76-1, April, 1976, Department of Aerospace Engineering, University Park, Pa.
3. Justus, C. G., et. al., "Four-D Global Reference Atmosphere Technical Description," Part I, NASA TM X-64871, September, 1974.
4. Justus, C. G., et. al., "Four- D Global Reference Atmosphere Technical Description," Part II, NASA TM X-64872, September, 1974.
5. Thomas, W. A., Introduction to Space Dynamics, John Wiley and Sons, Inc., New York, 1961, pp. 29-37, 107-113.

APPENDIX A

Satellite ParametersPrincipal Moments of Inertia

$$A = 7.93321 \times 10^5 \text{ kilograms-meter}^2$$

$$B = 3.767828 \times 10^6 \text{ kilograms-meter}^2$$

$$C = 3.694680 \times 10^6 \text{ kilograms-meter}^2$$

Aerodynamic Reference Area and Diameter

$$A_{\text{ref}} = 79.46 \text{ meter}^2$$

$$D_{\text{ref}} = 10.058 \text{ meter}^2$$

Density Reference Date and Time

March 1, 1980

12:00 noon

Julian Day = 2444301

Density Constants

$$417 \text{ kilometers } \omega_o = .06147591 \text{ seconds}^{-1}$$

$$\rho_B = 2.785 \times 10^{-12} \text{ kilogram/meter}^3$$

$$\rho_A = 1.295 \times 10^{-12} \text{ kilogram/meter}^3$$

$$370 \text{ kilometers } \omega_o = .0637886833 \text{ seconds}^{-1}$$

$$\rho_B = 6.3 \times 10^{12} \text{ kilogram/meter}^3$$

$$\rho_A = 2.55 \times 10^{12} \text{ kilogram/meter}^3$$

APPENDIX A (continued)

$$324 \text{ kilometers } \omega_o = .0646639997 \text{ seconds}^{-1}$$

$$\rho_B = 1.4975 \times 10^{-11} \text{ kilogram/meter}^3$$

$$\rho_A = 5.135 \times 10^{12} \text{ kilogram/meter}^3$$

$$287 \text{ kilometers } \omega_o = .0654498469 \text{ seconds}^{-1}$$

$$\rho_B = 3.9295 \times 10^{-11} \text{ kilogram/meter}^3$$

$$\rho_A = 1.0785 \times 10^{-11} \text{ kilogram/meter}^3$$

Initial Euler Angles

$$\psi = 1.07 \text{ degrees}$$

$$\theta = -79.96 \text{ degrees}$$

$$\phi = 12.85 \text{ degrees}$$

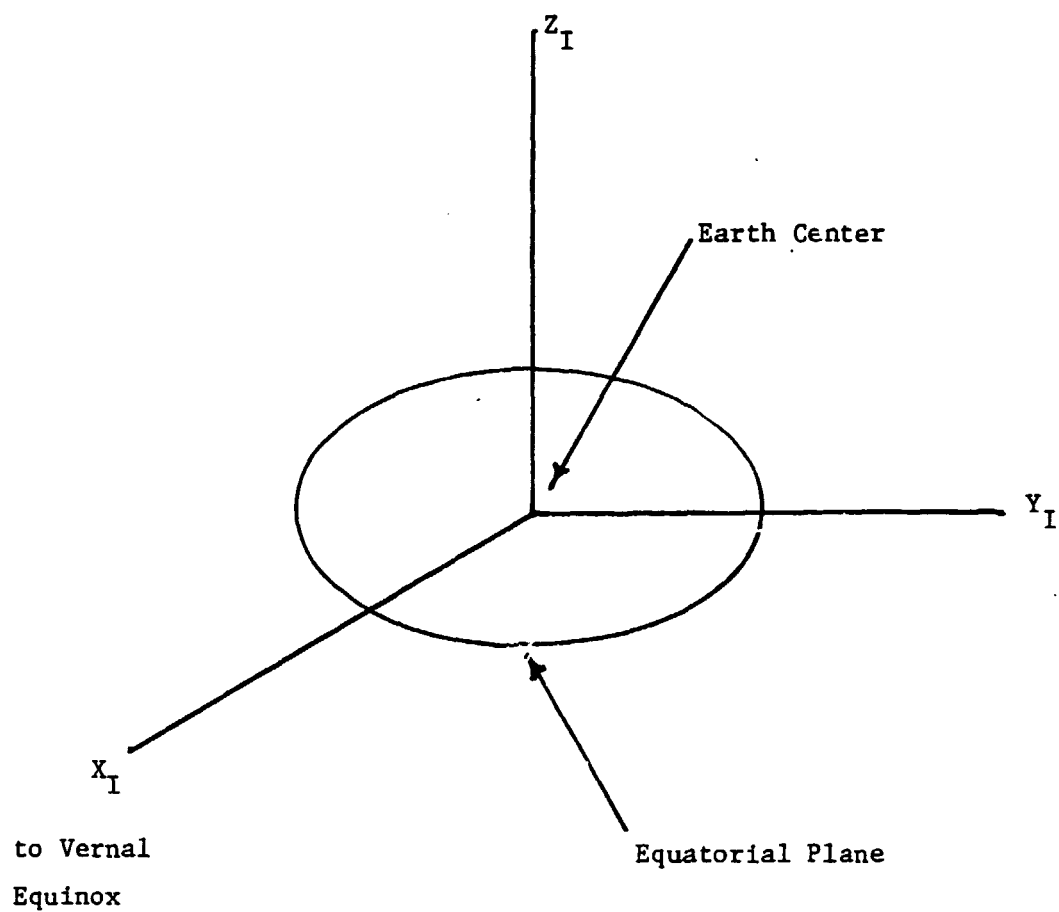


Figure 1. Geocentric Inertial Coordinate System

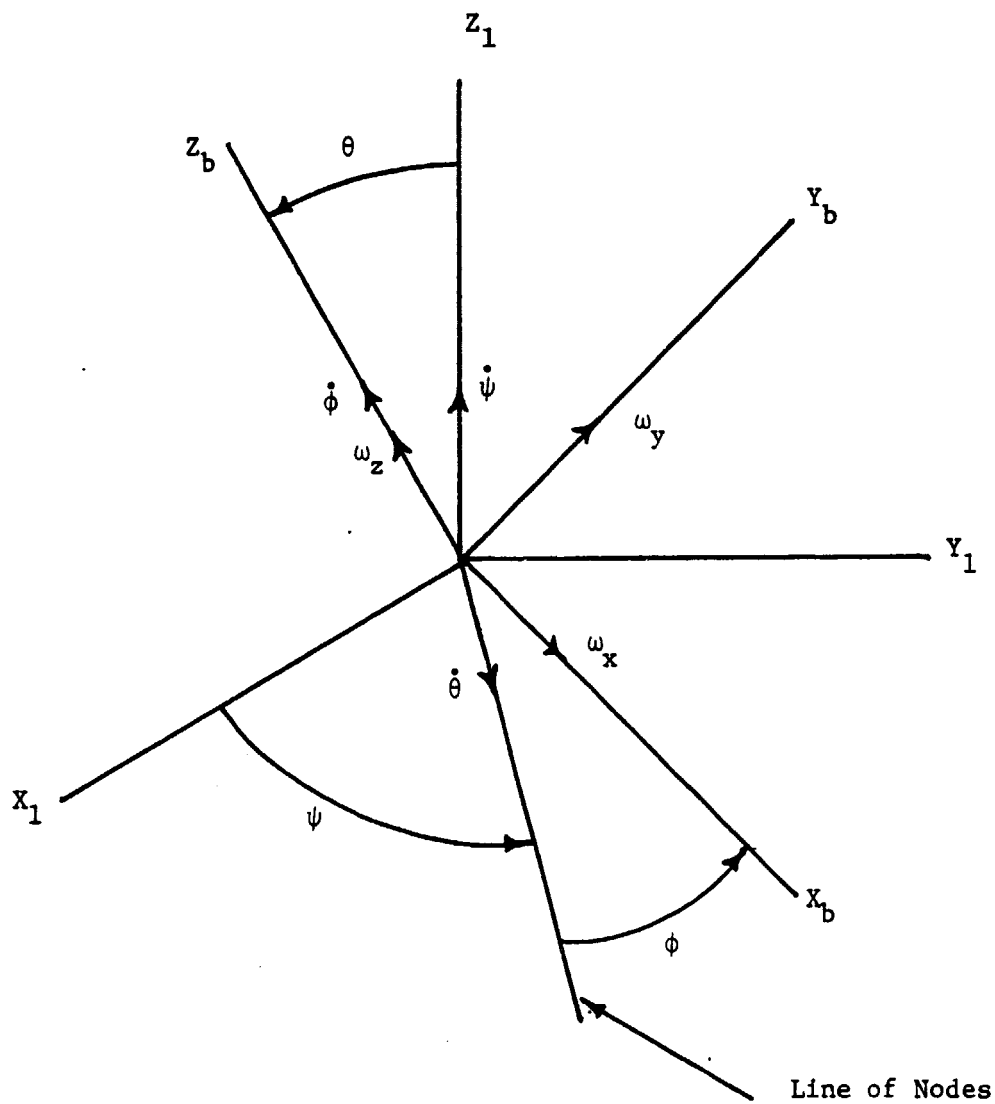


Figure 2. Euler angles, rates, and body rates

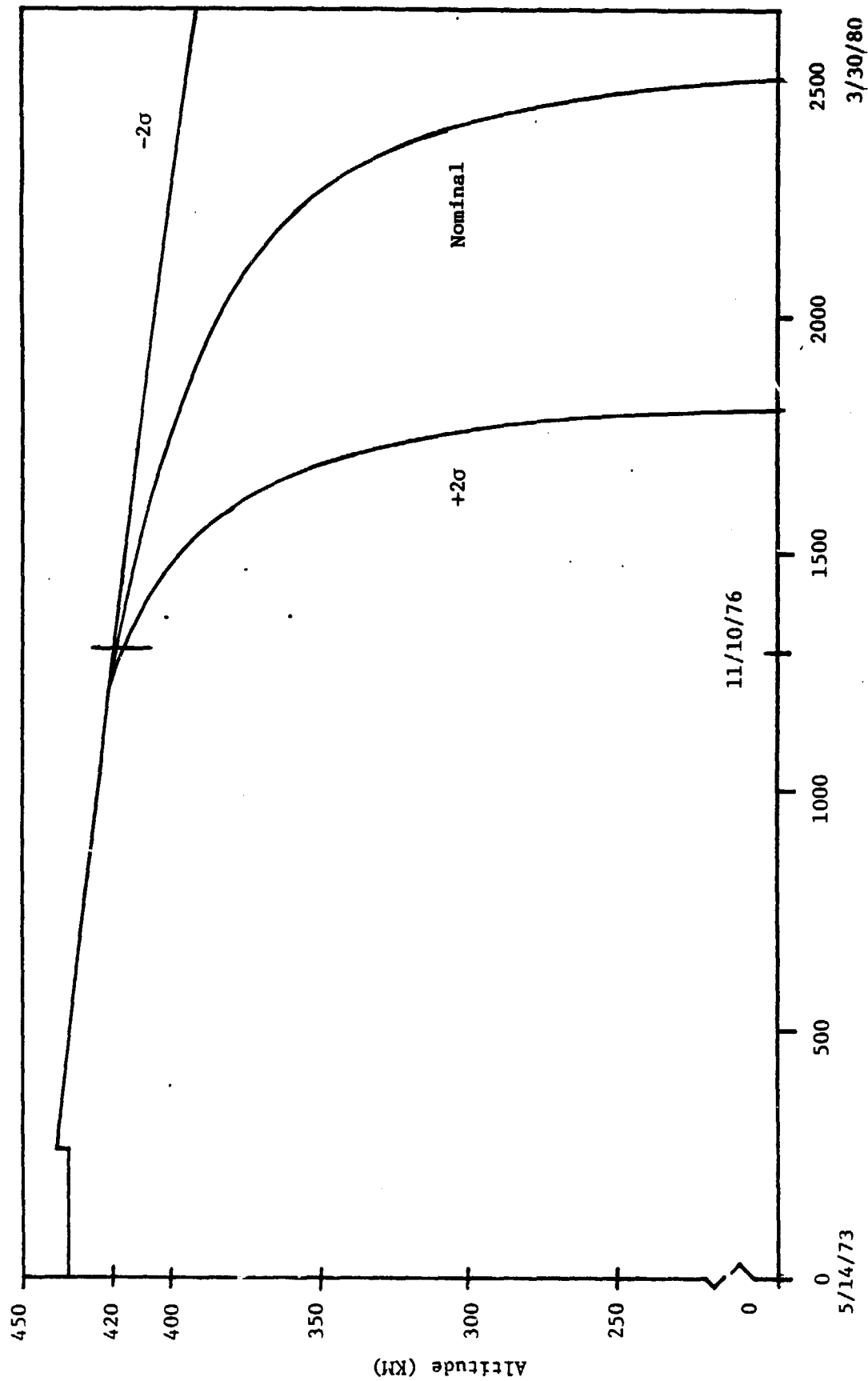


Figure 3. Skylab orbital decay

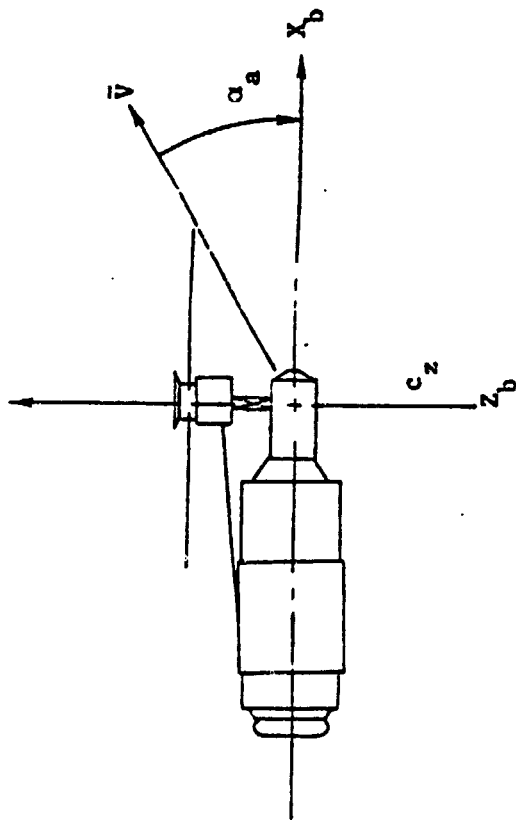
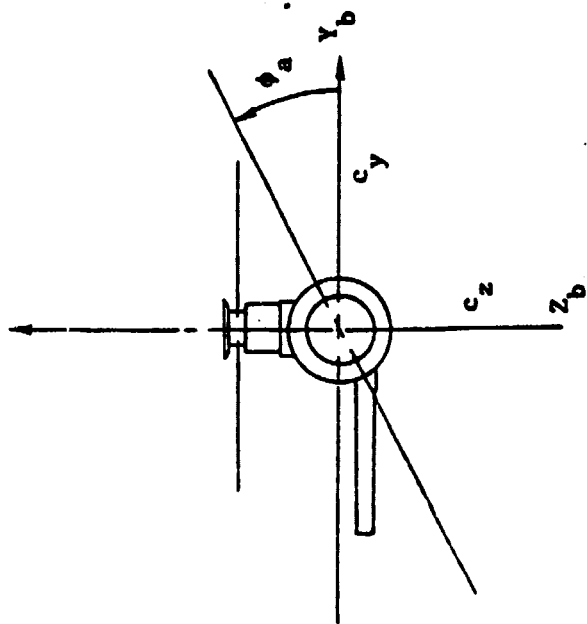
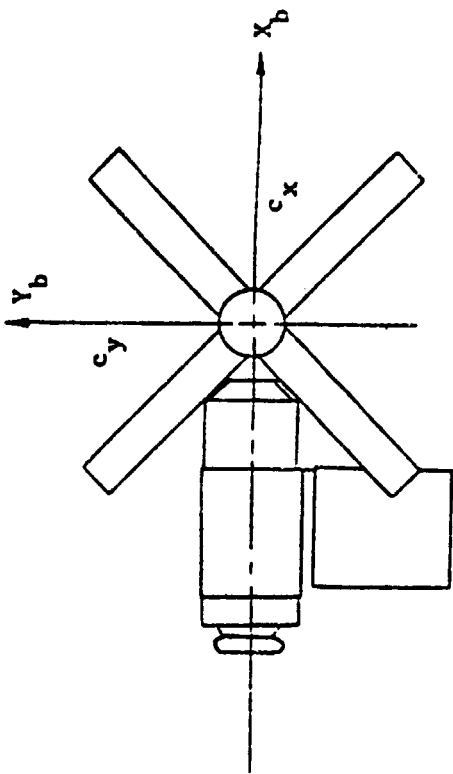


Figure 4. Skylab configuration for aerodynamic drag model

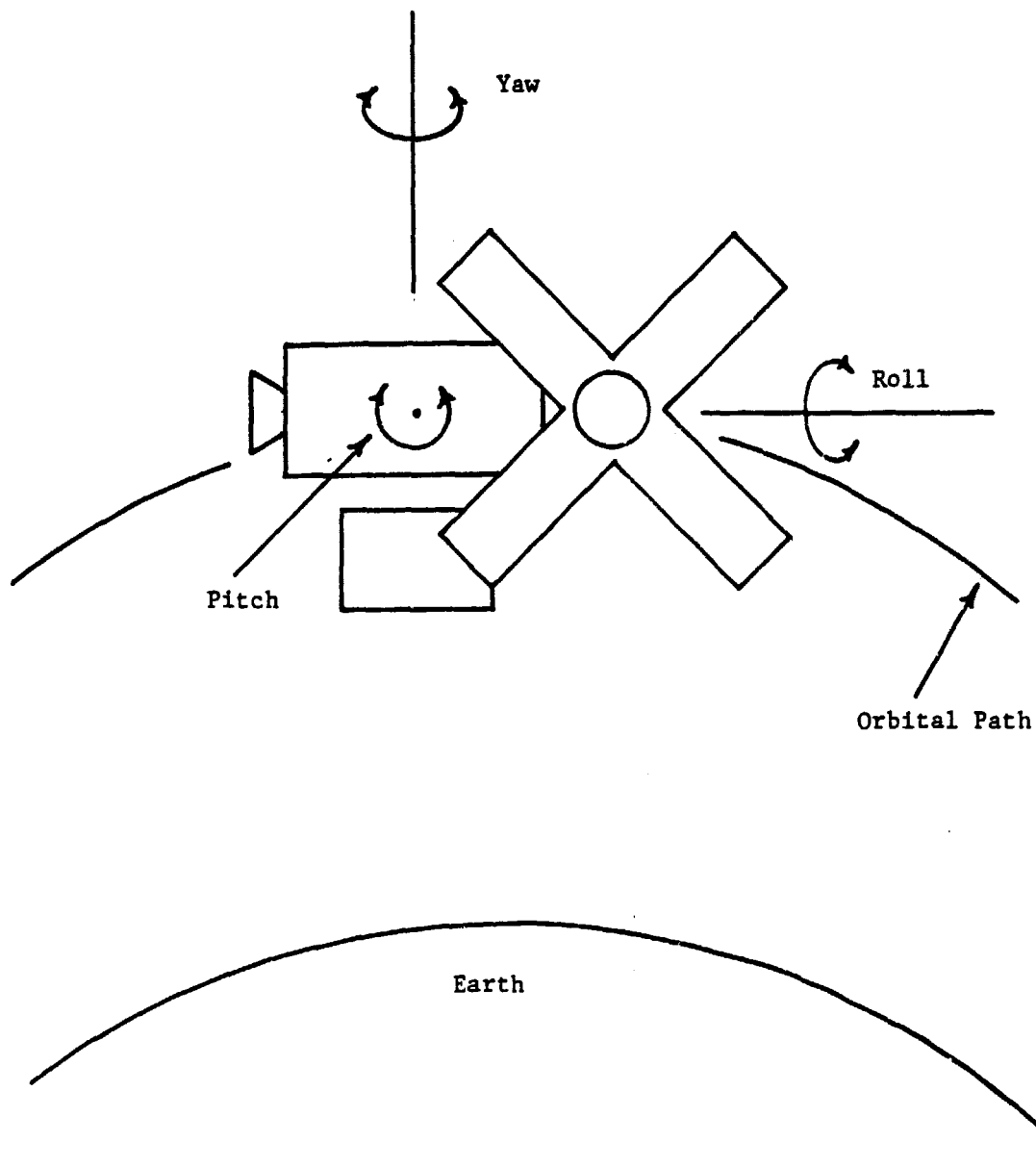


Figure 5. Pitch, roll, and yaw motion

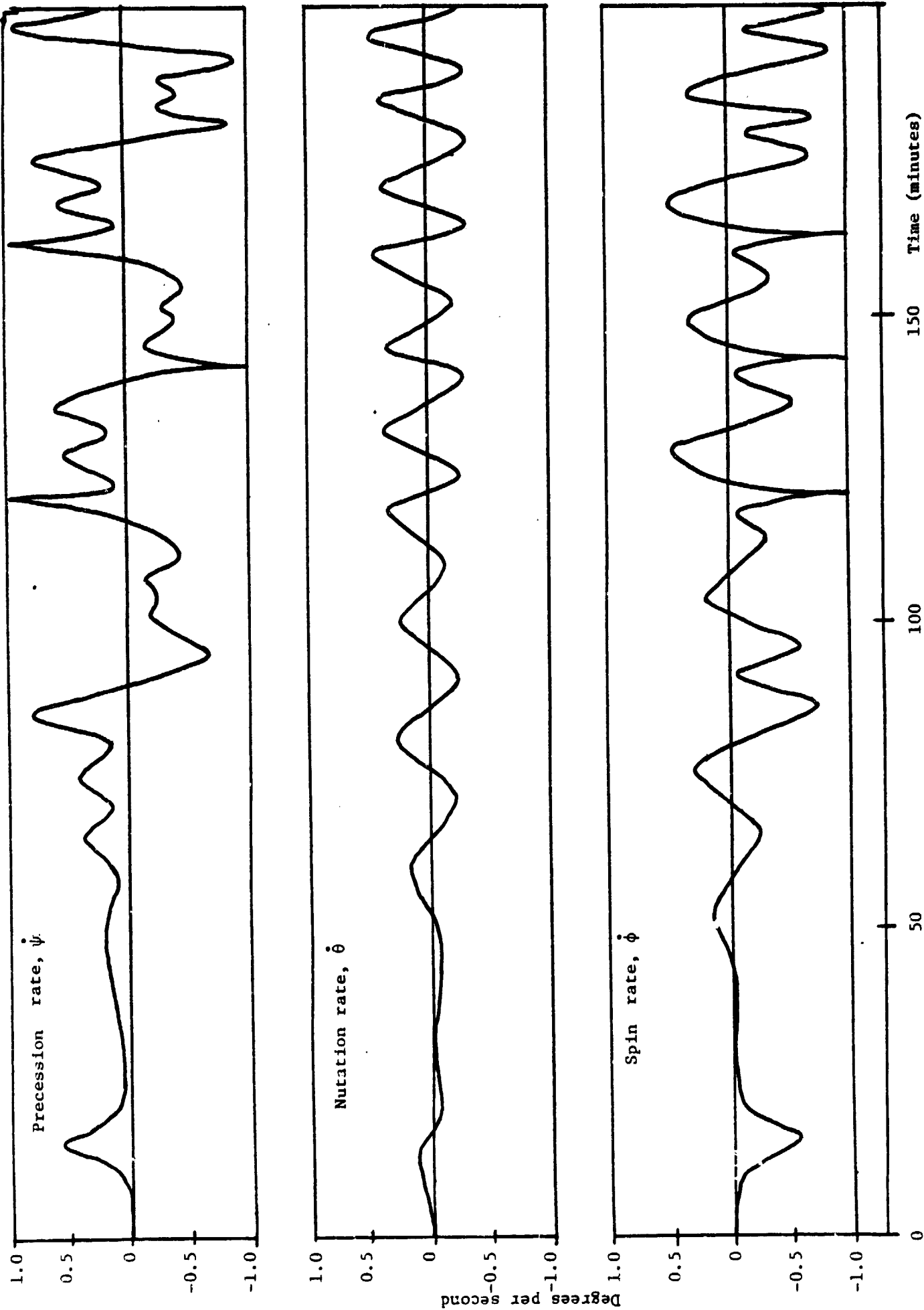


Figure 6. Precession, Nutation, and Spin Rates for 278 Kilometers

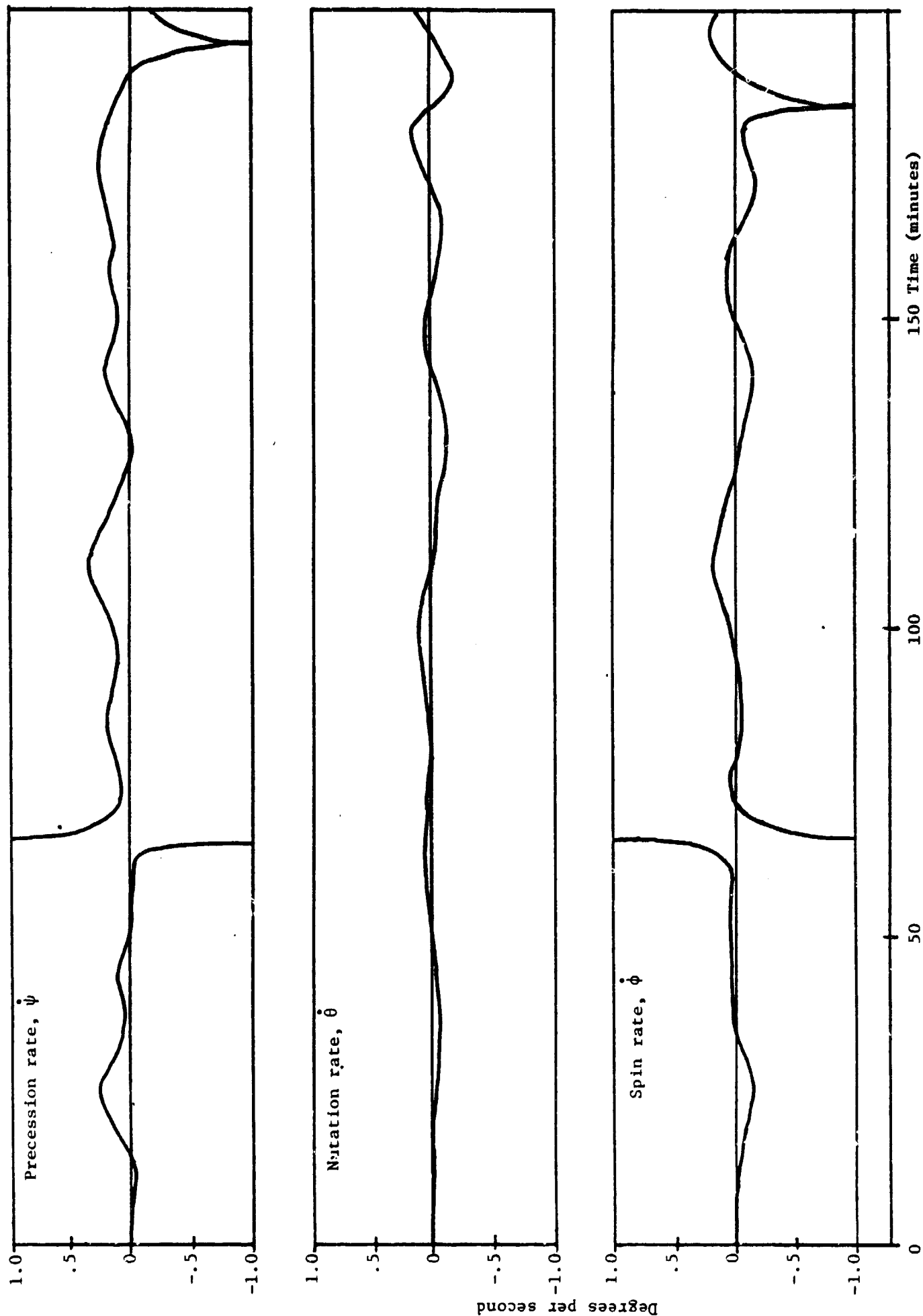


Figure 7. Precession, Nutation, and Spin rates for 324 kilometers

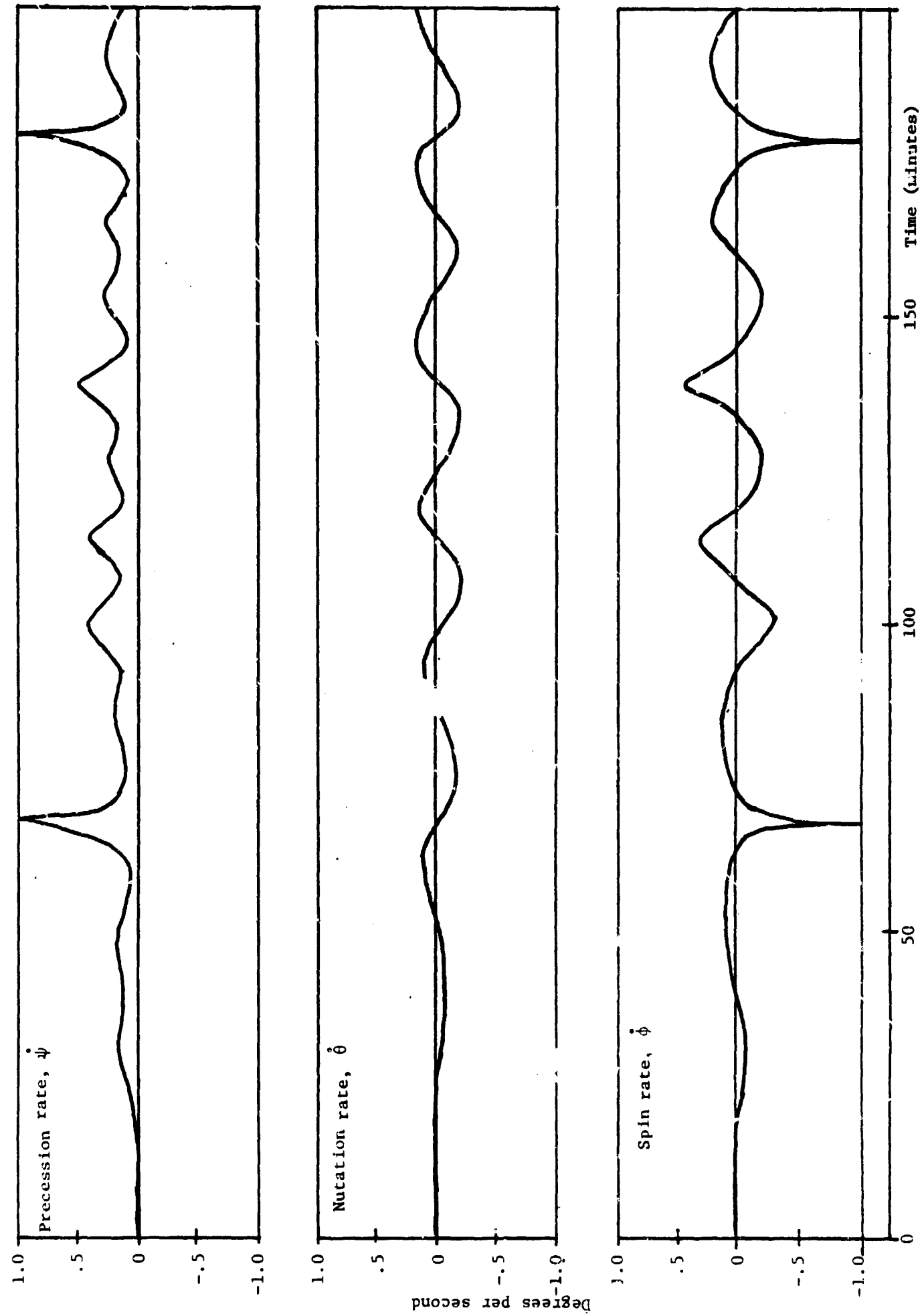


Figure 8. Precession, Nutation, and Spin rates for 370 kilometers

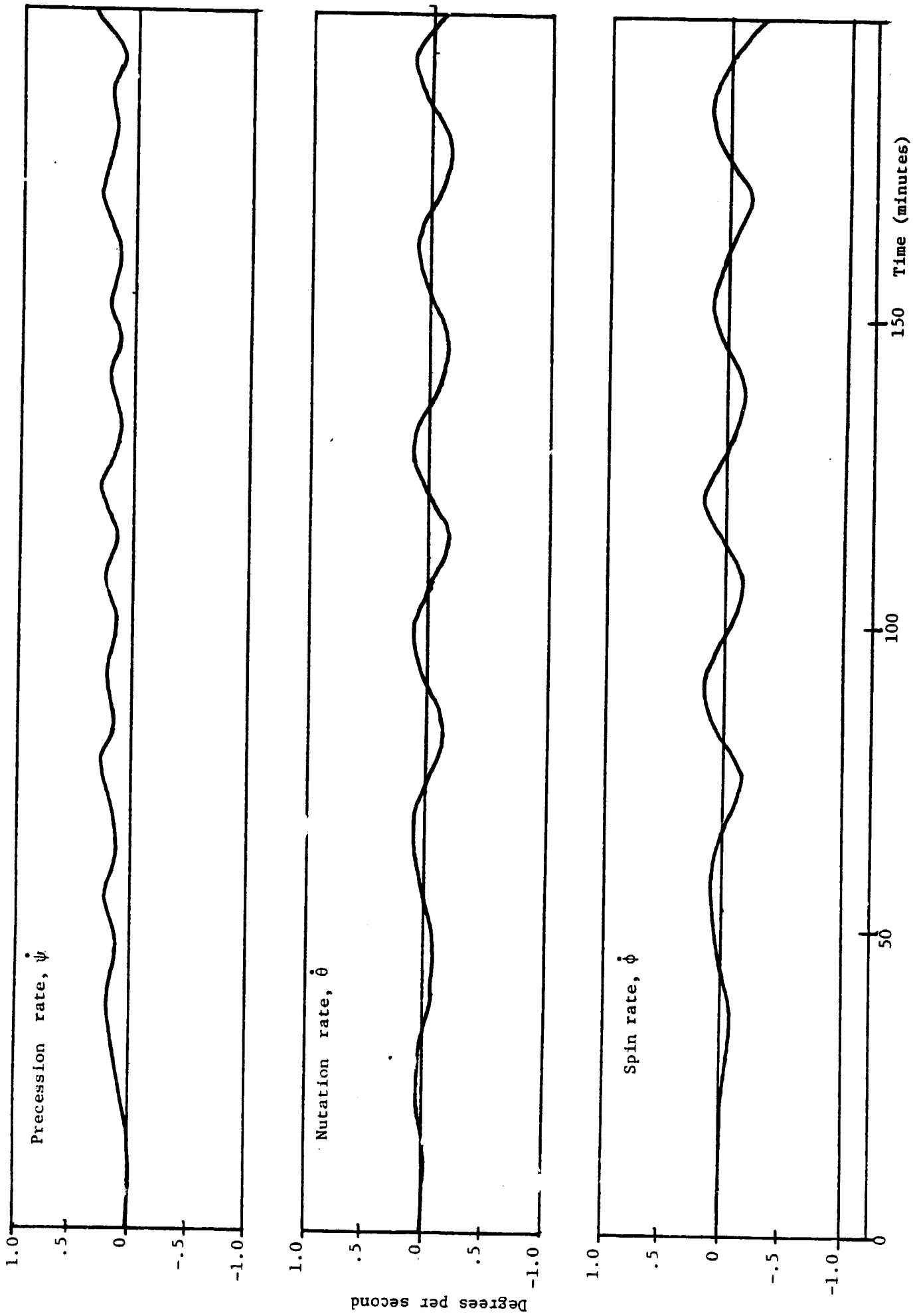


Figure 9. Precession, Nutation, and Spin rates for 417 kilometers

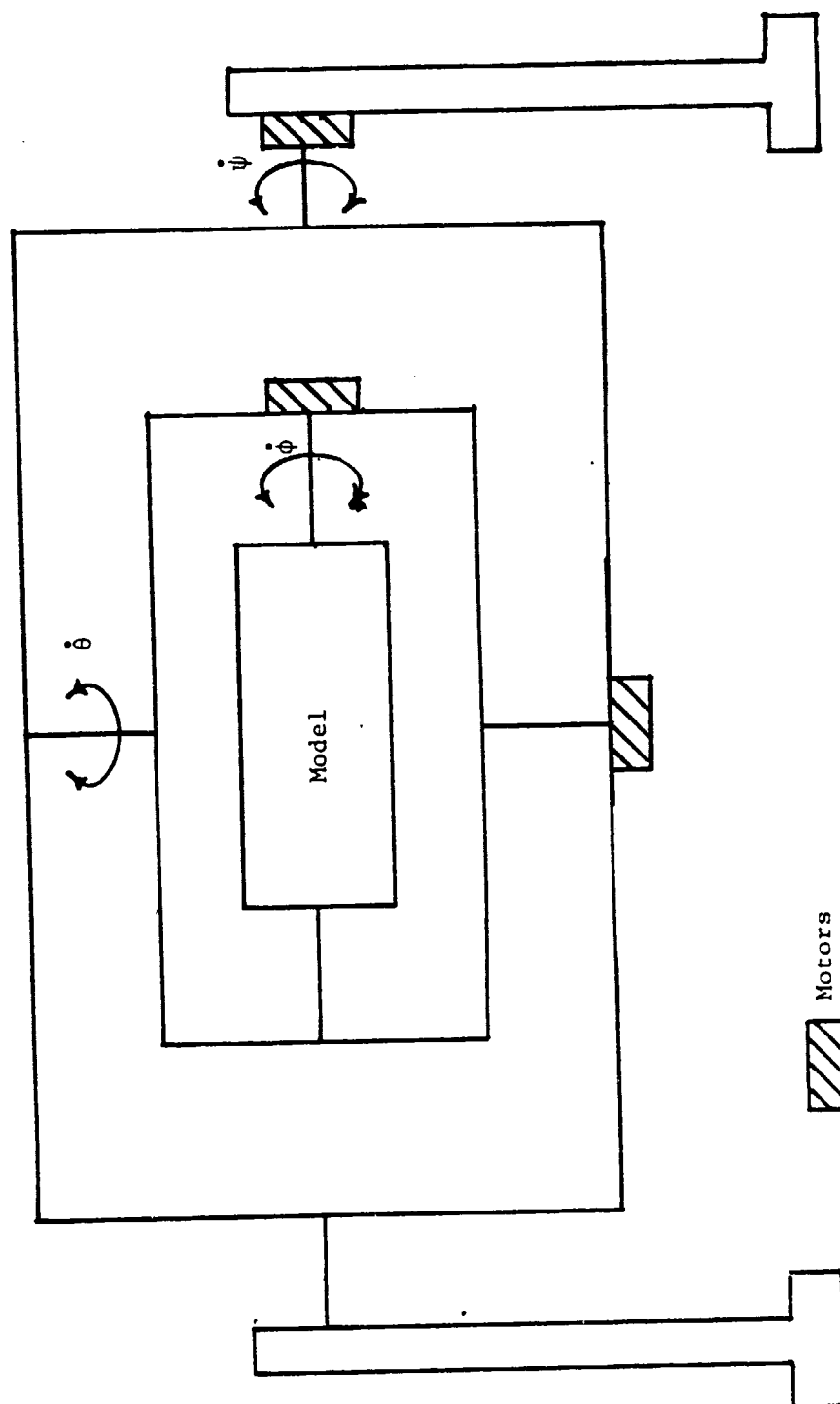


Figure 10. Simulator with Euler rates